DALTON

Synthesis, characterisation and crystal structure of 2-aminopyridinium (2-amino-5-bromopyridine)tribromocuprate(II) and bis(2-aminopyridinium) tetrabromocuprate(II)†

Antonio Luque, Jon Sertucha, Luis Lezama, Teófilo Rojo and Pascual Román*

Departamento de Química Inorgánica, Universidad del País Vasco, Apartado 644, E-48080 Bilbao, Spain

2-Aminopyridinium (2-amino-5-bromopyridine)tribromocuprate(II) **1** and bis(2-aminopyridinium) tetrabromocuprate(II) **2** have been prepared from acetonitrile solutions containing $CuBr_2$, HBr and 2-aminopyridine in 1:2:2 and 1:2:1 molar ratio, respectively. The mother-liquor of **1** was photoirradiated with a superhigh-pressure mercury lamp and the organic base underwent partial electrophilic *para* bromination of the substituted pyridine ring. The compounds have been characterised by elemental analysis, IR, UV/VIS and ESR spectroscopies, thermal analysis, variable-temperature magnetic susceptibility measurements and single-crystal X-ray diffraction. The crystal structure of **1** consists of infinite zigzag chains of $[C_5H_7N_2]^+$ cations and distorted $[CuBr_3(C_5H_5BrN_2)]^-$ tetrahedral anions running along the *b* axis and held together by means of N–H · · · Br hydrogen contacts and non-covalent interactions between the π systems of the pyridine rings. In **2** organic cations and flattened $[CuBr_4]^{2-}$ anions form two-dimensional N–H · · · Br hydrogen-bonded sheets which are connected by electrostatic interactions, van der Waals forces and face-to-face stacking interactions between the π systems of the aromatic cations. Magnetic susceptibility measurements of powdered samples showed that both compounds exhibit weak antiferromagnetic exchange interactions [$J = -1.20$ (**1**), -2.43 cm^{-1} (**2**)]. Thermal decomposition of both compounds yielded copper(II) oxide and metallic Cu as stable final residues in synthetic air and dinitrogen atmospheres, respectively.

The design and synthesis[1] of copper(II) halides continue to receive much attention owing to the wide variety of structural features of these compounds and their applications in fundamental and applied sciences ranging from solid-state physics to bioinorganic chemistry. Among solid-state physicists and chemists there is a great interest in the copper(II) halides owing to the plasticity of the metal co-ordination sphere which leads to a large variety of crystalline architectures with different co-ordination numbers, geometries and nuclearities,[2] and makes copper(II) systems excellent candidates for analysing correlations between structural parameters and magnetic properties.[3] In the biology field, recent studies have shown that several tetrahalogenocuprates(II) with substituted pyridinium cations exhibit potent gastroprotective activity[4] as well as antiepileptic effects.[5] These pharmacological works have also found that bromo complexes are significantly more active and show a lower cytotoxicity than the analogous chloro complexes. One of the best studied groups in the halogenocuprate(II) chemistry, both in solution and the solid state, are complexes of the type $[CuX_4]^{2-}$ (X = Br or Cl) with inorganic and organoammonium counter ions.[6] By contrast, as far as we are aware, species of the type $[HL][CuX_3L]$ (L = monodentate nitrogen base) are very scarce[7] and the only crystal structure containing bromide ligands published to date is that of the compound $[HL][CuBr_3L]$.[8] In an attempt to prepare new complexes of this type, during general research on copper(II) halide chemistry with aromatic nitrogen bases,[9] we have synthesized the compounds $[C_5H_7N_2][CuBr_3(C_5H_5BrN_2)]$ **1** and $[C_5H_7N_2]_2[CuBr_4]$ **2**. In **1** the 2-aminopyridine has two functions, it acts as a cation and as a monodentate N-donor ligand which has been brominated in the *para* position with respect to the amino substituent during a photoirradiation process.

† *Supplementary data available* (No. SUP 57207, 5 pp.): thermoanalytical data. See Instructions for Authors, *J. Chem. Soc., Dalton Trans.*, 1997, Issue 1.
Non-SI units employed: G = 10^{-4} T, $\mu_B \approx 9.27 \times 10^{-24}$ J T^{-1}.

Experimental

Reagents and physical measurements

All reagents were from Fluka and Merck, and used without further purification. Microanalyses for carbon, nitrogen and hydrogen were performed on a Perkin-Elmer CHN-2400 analyser; copper was determined by atomic absorption spectroscopy. The densities were measured by flotation in $CHBr_3$–CCl_4 mixtures.[10] Infrared spectra were recorded in the 4000–200 cm^{-1} range on an IR Perkin-Elmer 4200 spectrometer as KBr pellets, UV/VIS spectra using a Shimadzu 260 spectrometer for ethanol–HBr (48%) (20:1, v/v) solutions of the complexes in the region 190–900 nm. Simultaneous TG/DTG/DTA measurements were made in dynamic synthetic air and dry dinitrogen atmospheres with a Setaram Tag 24 S16 thermobalance and a heating rate of 5 °C min^{-1}. The enthalpy changes were quantitatively determined by a Mettler TA 4000 DSC instrument, with a sample weight of 5 mg and a heating rate of 5 °C min^{-1} in aluminium crucibles. X-Ray powder diffraction patterns of the compounds and the final products from the thermal decompositions were recorded at room temperature with a Philips PW 1710 instrument equipped with graphite-monochromated Cu-Kα radiation. The diffractograms of the residues were compared with those obtained from the ASTM powder diffraction files of the Joint Committee on Powder Diffraction Standards, JCPDS.[11] A Bruker ESP300 spectrometer, operating at X- (*ca.* 9.5) and Q-band (*ca.* 34 GHz) and equipped with a standard Bruker apparatus down to liquid-nitrogen and liquid-helium temperatures, was used to study the ESR polycrystalline spectra between 4.2 and 300 K. The magnetic susceptibility measurements were carried out on polycrystalline samples in the temperature range 4.2–300 K with a pendulum-type susceptometer/magnetometer (Manics DSM8) equipped with a helium continuous-flow cryostat. Diamagnetic correction terms were estimated from Pascal's constants[12] as -257×10^{-6} and -267×10^{-6} cm^3 mol^{-1} for **1** and **2**, respectively. Magnetic

susceptibility data were also corrected for temperature-independent paramagnetism (60×10^{-6} mol^{-1} per Cu^{II}) and magnetisation of the sample holder.

Preparations

$[C_5H_7N_2][CuBr_3(C_5H_5BrN_2)]$ 1. Polycrystalline samples of this compound were obtained as follows: concentrated hydrobromic acid (48%) (0.5 cm^3, 4.4 mmol) was added to an acetonitrile solution (10 cm^3) of 2-aminopyridine (0.42 g, 4.4 mmol). The reaction mixture was stirred at room temperature for 15 min. Initially a white solid was formed which was redissolved by heating to 60 °C. Later, copper(II) bromide (0.49 g, 2.2 mmol) dissolved in acetonitrile (20 cm^3) was added dropwise. The resulting black solution was filtered to remove any insoluble residue and then was irradiated for 6 h under an atmosphere of dinitrogen using an 500 W superhigh-pressure mercury lamp. The final solution was allowed to stand for slow evaporation at room temperature in a open atmosphere. After 2 d, a black polycrystalline solid appeared which was filtered off, washed with hexane and dried *in vacuo*. Yield 0.982 g, 78% based on copper (Found: C, 21.1; H, 2.2; Cu, 11.05; N, 10.0. Calc. for $C_{10}H_{12}Br_4CuN_4$: C, 21.0; H, 2.1; Cu, 11.1; N, 9.8%). IR (cm^{-1}): 3320s, 3300s, 3200s, 3150 (sh), 3020w, 1660vs, 1630vs, 1555m, 1395w, 1320w, 1265w, 1155w, 1095w, 830m, 760m, 715w, 635w, 550m, 450w and 295m. UV/VIS [EtOH–HBr, λ_{max}/nm (ε/dm^3 mol^{-1} cm^{-1})]: 555 (280), 305 (12 200), 270 (16 200) and 230 (14 700). X-Ray powder diffractogram (*d*/Å, relative intensities in parentheses): 7.102 (7), 6.907 (100), 4.948 (68), 4.172 (25), 3.867 (87), 3.521 (46), 3.242 (50), 3.152 (10), 2.924 (15), 2.893 (24), 2.703 (15) and 2.669 (20).

$[C_5H_7N_2]_2[CuBr_4]$ 2. This compound was synthesized as a microcrystalline product employing the above-described procedure except that a $CuBr_2$:HBr:2-aminopyridine molar ratio of 1:2:1 was used and the initial mixture was not photoirradiated. To a stirred acetonitrile solution of HBr (1 cm^3, 8.8 mmol) and 2-aminopyridine (0.42 g, 4.4 mmol) at 60 °C was added dropwise copper(II) bromide (0.98 g, 4.4 mmol). The resulting black solution was filtered off and then allowed to stand at room temperature. Overnight a black powder of **2** appeared. Yield 1.050 g, 45% based on copper (Found: C, 21.05; H, 2.4; Cu, 11.05; N, 9.75. Calc. for $C_{10}H_{14}Br_4CuN_4$: C, 20.95; H, 2.45; Cu, 11.1; N, 9.75%). IR (cm^{-1}): 3360s, 3295s, 3235w, 3185s, 3080w, 3015w, 2980w, 1660vs, 1620vs, 1540m, 1470s, 1380m, 1320m, 1225m, 1170m, 1080w, 990s, 760vs, 715s, 640w and 510s. UV/VIS [EtOH–HBr, λ_{max}/nm (ε/dm^3 mol^{-1} cm^{-1})]: 565 (500), 305 (17 200) and 230 (19 200). X-Ray powder diffractogram: 7.638 (35), 7.357 (65), 6.967 (22), 5.320 (18), 4.804 (67), 4.126 (42), 3.864 (40), 3.763 (10), 3.445 (24), 3.116 (100), 3.093 (28), 2.881 (15), 2.686 (15) and 2.457 (10) Å.

For both compounds, polyhedral dark violet crystals suitable for single-crystal X-ray crystallographic studies were grown by slow diffusion of hexane (20 cm^3) into an ethanol solution (5 cm^3) of the complexes (0.2 mmol) previously transferred to a glass tube (15 mm diameter). The crystals were filtered off, washed with diethyl ether and dried in a stream of dry dinitrogen. They were quite stable to light and X-ray exposure, but after 3 weeks lost crystallinity and gradually became a powder. All manipulations, except the photoirradiation process for compound **1**, were carried out in an open atmosphere. For both compounds the purity and homogeneity of the polycrystalline samples used for physical measurements were checked by IR spectroscopy, elemental analysis and by comparison of the observed X-ray powder diffraction patterns with those generated from the single-crystal X-ray data.[13]

Crystallography

Crystals of dimensions 0.10 × 0.15 × 0.20 (complex **1**) and 0.30 × 0.35 × 0.50 mm (**2**) were mounted on an Enraf-Nonius CAD4 four-circle diffractometer and used for data collections. The unit-cell parameters were determined from automatic centering of 25 reflections ($7 < \theta < 15°$) and refined by the least-squares method. Intensity data were collected at room temperature by using graphite-monochromated Mo-Kα radiation ($\lambda = 0.710\,69$ Å) with the ω–2θ scan mode. Information concerning crystal parameters and structure refinements is summarised in Table 1. Intensity data were collected for Lorentz-polarisation and absorption[14] effects. Atomic scattering factors and anomalous dispersion terms were taken from ref. 15. The structures were solved by direct methods[16] and refined (on *F*) by full-matrix least squares using the X-RAY 76 program package[17] on a MicroVAX II computer. Non-hydrogen atoms were refined anisotropically, except for two cation carbon atoms of **1** which were refined isotropically due to their considerably high thermal motion. The enlarged thermal ellipsoids for some of the atoms of the cation in **1** reflect the 'smeared out' electron density resulting from the thermal disorder. The largest peak in the final Fourier-difference map of **1**, about 1.22 e Å^{-3} high, was located in the vicinity of the cation atoms. All hydrogen atoms were generated geometrically, except those at nitrogen atoms of compound **2** obtained from a Fourier-difference synthesis map and isotropically refined. A convenient weighting scheme[18] was used in final cycles of refinement to obtain flat dependence in $\langle w\Delta^2F \rangle$ *vs.* $\langle F_o \rangle$ and $\langle \sin\theta/\lambda \rangle$. Models reached convergence with values of *R* and *R′* listed in Table 1. The residual maxima and minima in the final Fourier-difference maps were 0.83 and −0.90 e Å^{-3} for **1** and 1.22 and −0.89 e Å^{-3} for **2**. The molecular plots were drawn with the PLATON program.[19]

Atomic coordinates, thermal parameters and bond lengths and angles have been deposited at the Cambridge Crystallographic Data Centre (CCDC). See Instructions for Authors, *J. Chem. Soc., Dalton Trans.*, 1997, Issue 1. Any request to the CCDC for this material should quote the full literature citation and the reference number 186/359.

Results and Discussion

Synthesis and chemical characterisation

Elemental analysis alone cannot distinguish between $[C_5H_7N_2][CuBr_3(C_5H_5BrN_2)]$ **1** and $[C_5H_7N_2]_2[CuBr_4]$ **2**, the later showing two non-brominated aromatic cations. Moreover, the IR and UV/VIS spectra do not provide any conclusive evidence in favour of the co-ordination of the base and the pyridine-ring bromination in **1**. Although the IR spectrum of **1** shows two weak bands at 550 and 295 cm^{-1} which might be attributable to the C–Br and Cu–N stretching vibrations, respectively, the remaining peaks correspond to the aromatic 2-aminopyridine species and are quite similar to those found for compound **2**. The UV/VIS spectra of both compounds are also quite similar, showing a strong band at 230 nm which corresponds to the $\pi \longrightarrow \pi^*$ and $n \longrightarrow \pi^*$ transitions at the pyridinic rings,[20] and two bands at 305 and *ca.* 560 nm which are associated with ligand-to-metal charge-transfer transitions, since, according to the literature, the d–d transitions are expected in the near-IR region.[21,22] The weak broad bands at around 560 nm are responsible for the dark violet colour and metallic lustre of both compounds. A band at 270 nm is observed in the spectrum of **1** which is not present in that of **2** and is probably due to the occurrence of both cationic and co-ordinated aromatic species in **1**. However, the X-ray powder diffractograms of both compounds are significantly different and clearly show that **1** and **2** are two different species. This assumption was also supported by the experimental density measurements which proved to be useful to detect the two compounds; the density of **1** ($D_m = 2.35$ g cm^{-3}) is significantly higher than that corresponding to **2** ($D_m = 2.21$ g cm^{-3}). Consequently, taking into account all these data, single-crystal structure determinations of **1** and **2** were

Table 1 Summary of crystal data[a] for $[C_5H_7N_2][CuBr_3(C_5H_5BrN_2)]$ **1** and $[C_5H_7N_2]_2[CuBr_4]$ **2**

	1	**2**
Formula	$C_{10}H_{12}Br_4CuN_4$	$C_{10}H_{14}Br_4CuN_4$
M	571.39	573.41
Crystal system	Monoclinic	Triclinic
Space group	$P2_1/n$	$P\bar{1}$
a/Å	7.739(1)	8.090(1)
b/Å	13.814(1)	8.366(1)
c/Å	15.186(1)	14.020(1)
α/°		91.23(1)
β/°	94.25(2)	95.22(1)
γ/°		113.82(1)
U/Å^3	1619.0(3)	862.7(2)
Z	4	2
D_c/g cm^{-3}	2.341	2.207
D_m/g cm^{-3}	2.35(1)	2.21(1)
μ(Mo-Kα)/cm^{-1}	111.26	104.40
F(000)	1076	542
No. measured reflections	4662	5040
No. of observed reflections,[b] N_o	1652	2493
No. of parameters, N_p	162	172
Goodness of fit[c]	1.25	1.24
R[d]	0.048	0.042
R'[e]	0.047	0.045

[a] Details in common: $T = 295(1)$ K, θ 1–30°. [b] $I \geqslant 2\sigma(I)$. [c] $[\Sigma w(|F_o| - |F_c|)^2/(N_o - N)]^{\frac{1}{2}}$. [d] $\Sigma||F_o| - |F_c||/\Sigma|F_o|$. [e] $[\Sigma w(|F_o| - |F_c|)^2/\Sigma w|F_o|^2]^{\frac{1}{2}}$.

undertaken in order to determine unambiguously their exact stoichiometry and the actual structures.

An interesting feature of compound **1** is the bromination of the pyridine ring of the ligand. Bromination processes have been also observed in the reaction of a $CuBr_2$–HBr mixture with 2-amino-*n*-methylpyridine ($n = 3$, 5, 6)[23] or 3-aminopyridine.[24] In the latter reaction the bromination process is tied to reduction of copper-(II) to -(I) and a mixed-valence Cu^ICu^{II} system is obtained. Indeed, it has been suggested that the bromination process is due to decomposition of $CuBr_2$ to CuBr and Br_2 which is improved by the existence of a high excess of $CuBr_2$. Although pyridine is normally resistant to electrophilic substitution, the substituting *exo*-amino groups activate the ring toward a *para* bromination which is readily achieved in the presence of Br_2 under mildly acidic conditions. In our work, compound **1** does not contain copper(I) and the amount of copper(II) bromide used in its preparation is less than that employed for the synthesis of **2**. Therefore, in our case, the decomposition of starting $CuBr_2$ to CuBr and Br_2 with the consequent bromination of a part of the organic base to yield 2-amino-5-bromopyridine should be induced by the photoirradiation process. The non-existence of copper(I) in **1** is due to the air oxidation of Cu^I to Cu^{II} when the irradiated solution was allowed to stand at room temperature in an open atmosphere.

Crystal structures

$[C_5H_7N_2][CuBr_3(C_5H_5BrN_2)]$ 1. This crystal structure consists of $[CuBr_3(C_5H_5BrN_2)]^-$ complex anions and 2-aminopyridinium cations which are linked together by means of electrostatic forces, N–H···Br hydrogen bonds and face-to-face interactions between the π systems of the aromatic rings. Fig. 1 shows the asymmetric unit of this compound together with the atomic numbering scheme. Table 2 lists selected bond lengths and angles together with the hydrogen contacts.

The copper(II) ion is bound to three bromine atoms and to the *endo*-nitrogen atom of the 2-amino-5-bromopyridine ligand. The Cu–Br (mean 2.378 Å) and Cu–N (1.993 Å) distances are within the range observed in analogous complexes.[8] The chromophore $CuBr_3N$ presents a distorted tetrahedral geometry with two bond angles (133.5 and 136.7°) distinguished from the rest (mean 98.4°), and showing that the geometry is intermediate between square-planar (D_{4h}) and regular tetrahedral (T_d). The distortion from tetrahedral geometry has been evaluated by application of the Muetterties and Guggenberger method,[25] which by considering the dihedral angles between the various faces of the polyhedron leads to a measure of the polytopal shape by reference to idealised geometries ($\Delta D = 0$ for a regular tetrahedron and 100 for a D_{4h} geometry). The value obtained, $\Delta D = 25.1\%$, indicates that the anion is not much distorted from regular tetrahedral geometry but is higher than that found for the compound $[Hmt][CuBr_3(mt)]$[8] [mt = 5-(2-hydroxyethyl)-4-methyl-3-thiazole] ($\Delta D = 18.5\%$) probably due to the existence of stronger hydrogen bonds in **1**.

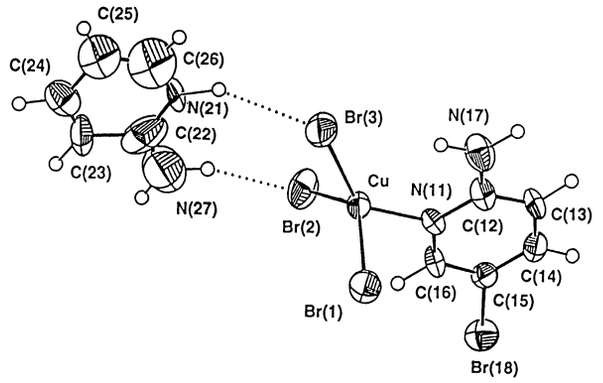

Fig. 1 Thermal ellipsoid plot (50% probability level) of the asymmetric unit of $[C_5H_7N_2][CuBr_3(C_5H_5BrN_2)]$ **1** with the labelling scheme

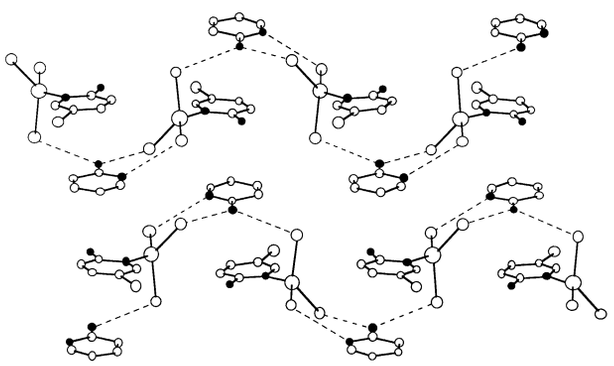

Fig. 2 Arrangement of anionic complexes and organic cations in the crystal structure of complex **1** forming N–H···Br hydrogen-bonded chains. Hydrogen atoms are omitted for clarity

As far as the organic ligand and the cation is concerned, they are planar [deviation from the average plane: 0.049(1) Å for Br(18) and 0.030(1) Å for N(25)] and their bond lengths and angles are comparable to those previously reported for substituted pyridine rings.[26] The relatively large atomic thermal parameters and the presence of several anomalous bond distances and angles in the organic cation suggest, as stated earlier, either significant thermal motion or the existence of some disorder within the cation.

In the crystal structure, anions (*a*) and cations (*c*) are stacked forming infinite zigzag one-dimensional chains along the *b* axis direction with a ... *acac* ... sequence (Fig. 2). In these chains the units are held together by means of N–H···Br hydrogen-bonding network in which both the ammonium and amino groups of the cations are donors and the three bromine atoms of the anion are acceptors (see end of Table 2). The closest Cu···Cu distance (7.048 Å) in the structure is found between adjacent anions in the hydrogen-bonded chain. The amino and bromo substitutents of the 2-amino-5-bromopyridine ligand point towards the outer of the chain, presumably to minimise electrostatic interactions and steric hindrances. The C–Br and C–N bonds are nearly perpendicular (*ca.* 72°) to the propagation direction of the ... *acac* ... chain which precludes the involvement of the ligand substituents in any significant

Table 2 Selected bond distances (Å), angles (°) and hydrogen-bonding system (Å,°) for compound **1** with estimated standard deviations (e.s.d.s) in parentheses

Copper environment

Cu–Br(1)	2.402(1)	Cu–Br(3)	2.347(2)	Br(1)–Cu–Br(2)	133.52(7)	Br(2)–Cu–Br(3)	99.38(6)
Cu–Br(2)	2.385(2)	Cu–N(11)	1.993(6)	Br(1)–Cu–Br(3)	101.80(6)	Br(2)–Cu–N(11)	96.6(2)
				Br(1)–Cu–N(11)	95.6(2)	Br(3)–Cu–N(11)	136.7(2)

Aromatic ligand ($X = 1$) and cation ($X = 2$)

	$X = 1$	$X = 2$		$X = 1$	$X = 2$
N(X1)–C(X2)	1.34(1)	1.43(3)	C(X2)–N(X1)–C(X6)	119.1(6)	122(2)
N(X1)–C(X6)	1.33(1)	1.20(3)	N(X1)–C(X2)–C(X3)	122.4(8)	116(1)
C(X2)–C(X3)	1.37(1)	1.44(3)	N(X1)–C(X2)–N(X7)	117.4(7)	127(2)
C(X2)–N(X7)	1.37(1)	1.20(3)	C(X3)–C(X2)–N(X7)	120.3(8)	117(2)
C(X3)–C(X4)	1.40(1)	1.30(2)	C(X2)–C(X3)–C(X4)	117.4(8)	115(1)
C(X4)–C(X5)	1.36(1)	1.53(2)	C(X3)–C(X4)–C(X5)	119.0(8)	126(1)
C(X5)–C(X6)	1.35(1)	1.25(3)	C(X4)–C(X5)–C(X6)	120.0(8)	109(2)
C(X5)–Br(X8)	1.890(9)		N(X1)–C(X6)–C(X5)	122.2(7)	132(2)
			C(X6)–C(X5)–Br(X8)	118.4(6)	
			C(X4)–C(X5)–Br(X8)	121.6(6)	

Hydrogen-bond type*	N ··· Br	H ··· Br	N–H ··· Br
N(21)–H(211) ··· Br(3^{I})	3.50(1)	2.59	151
N(27)–H(271) ··· Br(1^{II})	3.64(2)	2.70	175
N(27)–H(272) ··· Br(2^{I})	3.42(2)	2.47	159

* Symmetry codes: I $-x + 1, -y + 1, -z$; II $x + \frac{1}{2}, -y + \frac{3}{2}, z - \frac{1}{2}$.

Table 3 Selected bond distances (Å), angles (°) and hydrogen-bonding system (Å,°) for compound **2** with e.s.d.s in parentheses

Anion

Cu–Br(1)	2.394(1)	Cu–Br(3)	2.362(1)	Br(1)–Cu–Br(2)	99.69(5)	Br(2)–Cu–Br(3)	100.13(5)
Cu–Br(2)	2.374(1)	Cu–Br(4)	2.365(1)	Br(1)–Cu–Br(3)	130.17(5)	Br(2)–Cu–Br(4)	134.89(5)
				Br(1)–Cu–Br(4)	98.63(5)	Br(3)–Cu–Br(4)	98.74(5)

Cations

	$X = 1$	$X = 2$		$X = 1$	$X = 2$
N(X1)–C(X2)	1.34(1)	1.34(1)	C(X2)–N(X1)–C(X6)	123.5(5)	121.6(6)
N(X1)–C(X6)	1.37(1)	1.35(1)	N(X1)–C(X2)–N(X7)	119.7(5)	118.5(7)
C(X2)–C(X3)	1.41(1)	1.39(1)	N(X1)–C(X2)–C(X3)	117.0(5)	118.8(6)
C(X2)–N(X7)	1.33(1)	1.33(1)	C(X3)–C(X2)–N(X7)	123.3(5)	122.7(7)
C(X3)–C(X4)	1.35(1)	1.36(1)	C(X2)–C(X3)–C(X4)	120.3(6)	119.5(7)
C(X4)–C(X5)	1.45(1)	1.41(1)	C(X3)–C(X4)–C(X5)	120.3(7)	121.0(7)
C(X5)–C(X6)	1.33(1)	1.35(1)	C(X4)–C(X5)–C(X6)	118.9(6)	116.9(7)
			N(X1)–C(X6)–C(X5)	120.1(5)	122.3(7)

Hydrogen-bond type*	N ··· Br	H ··· Br	N–H ··· Br
N(11)–H(11) ··· Br(4^{I})	3.37(1)	2.58(6)	139(4)
N(17)–H(171) ··· Br(4^{II})	3.47(1)	2.48(7)	167(5)
N(17)–H(172) ··· Br(2^{I})	3.45(1)	2.45(8)	169(5)
N(21)–H(21) ··· Br(2)	3.31(1)	2.30(6)	164(4)
N(27)–H(271) ··· Br(1^{III})	3.48(1)	2.47(6)	175(5)
N(27)–H(272) ··· Br(3)	3.42(1)	2.43(7)	163(5)

* Symmetry codes: I $x + 1, y, z$; II $x + 1, y + 1, z$; III $-x, -y, -z$.

intra- or inter-hydrogen bonding. The cohesiveness of the one-dimensional chains is also ensured by a face-to-face non-covalent interaction between π systems of the pyridine rings of the ligand and the cation. The dihedral angles between the rings, which are staggered in order to avoid steric hindrances, is 3.5°, the interplanar distance is 3.51 Å, the lateral offset is 1.70 Å, and interatomic distances range from 3.48 to 3.70 Å. The aromatic ligand and cation of two neighbouring chains are also almost parallel stacked with a dihedral angle of 7.2° and an interplanar separation of 3.44 Å, but are largely offset one from another (2.78 Å) which seems to indicate only a very slight overlapping, so that it is quite likely that the interchain interaction is only due to electrostatic effects.

$[C_5H_7N_2]_2[CuBr_4]$ 2. In the structure of this compound the discrete $[CuBr_4]^{2-}$ anions and the 2-aminopyridinium cations are stacked forming corrugated sheets in which the units are linked together by means of a two-dimensional network of N–H ··· Br hydrogen bonds. A perspective view of the asymmetric unit is depicted in Fig. 3. Selected bond lengths and angles and hydrogen contacts are listed in Table 3.

In the sheets (Fig. 4) the hydrogen atoms of both *endo*- and *exo*-amino groups of the cations point towards the bromine atoms of the anions to form N–H ··· Br hydrogen bonds, and as a consequence the outer border of the sheets is occupied by the carbon atoms of the pyridine rings. Through this the cohesiveness between sheets along the *c* axis is achieved by means of weak van der Waals interactions between the carbon atoms of the cation X(1) [Fig. 4(*a*)]. On the other hand, the two crystallographically independent 2-aminopyridinium cations are non-coplanar and the cation X(1) mean plane forms a dihedral angle of 61° with the cation X(2). This arrangement permits

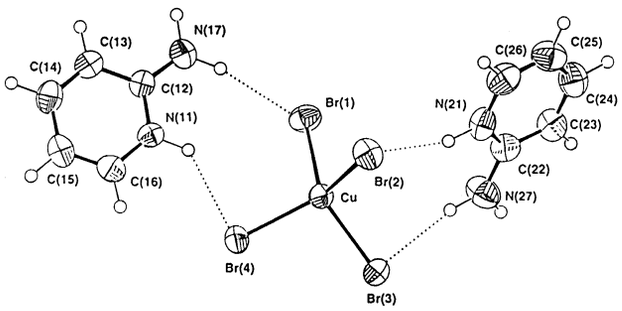

Fig. 3 Asymmetric unit of $[C_5H_7N_2]_2[CuBr_4]$ **2** with the labelling scheme

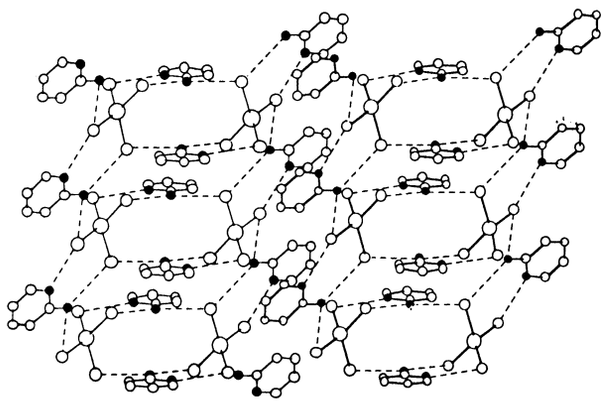

(*a*)

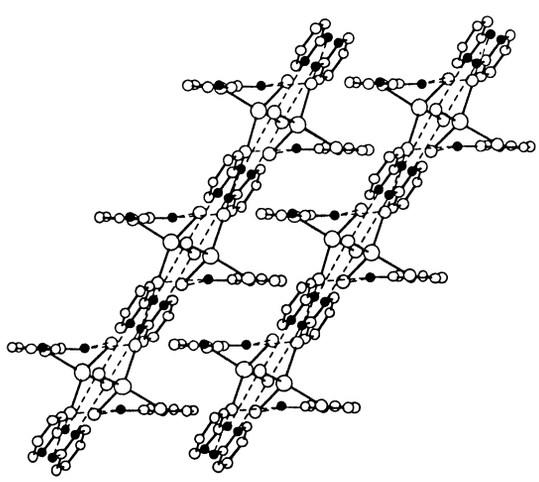

(*b*)

Fig. 4 Two hydrogen-bonded anion–cation sheets held together by van der Waals forces (*a*) and by π–π interactions (*b*) in the crystal structure of compound **2**

neighbouring two-dimensional hydrogen-bonding sheets to be connected along the *a* axis by partial overlapping of two cations belonging to each sheet, as shown in Fig. 4(*b*): the dihedral angle between the rings is 0°, the interplanar separation 3.52 Å and the lateral offset 1.56 Å. There are no other important interactions in the crystal structure, the shortest metal–metal separation being 6.85 Å between two tetrabromocuprate(II) anions belonging to neighbouring sheets. The shortest Br(1)···Br(3) contact (4.13 Å), from adjacent anions lying on the same sheet, is 0.23 Å longer than the sum of the bromine ion van der Waals radii (3.90 Å).

As far as the geometry of the $[CuBr_4]^{2-}$ anion is concerned, the Cu–Br bond lengths are in the range 2.36–2.39 Å, similar to those usually found for analogous compounds.[2,6,22,23] The Br–Cu–Br bond angles vary within the range 98.7–134.9°, revealing a highly flattened geometry. The distortion, $\Delta D = 21.1\%$, is at the higher end of the range previously observed for isolated tetrabromocuprate(II) anions.[8] A semi-empirical molecular orbital study of the T_d–D_{4h} equilibrium in tetrabromometal complexes[27] indicated that the $[CuBr_4]^{2-}$ anion has a tendency to display the T_d configuration, but it has been proposed that strong hydrogen bonds involving the bromine atoms remove charge from the bromide ions and favour distortion to D_{2d} symmetry.[28] In fact, most of the compounds which involve organic cations are able to form an extensive hydrogen-bond network, which influences the Cu–Br bond lengths and Br–Cu–Br angles and leads to a compressed tetrahedral configuration with a near D_{2d} symmetry of the anion. Table 4 shows the distortion ΔD from a regular tetrahedral geometry observed for some halogenocuprate(II) complexes. Muetterties distortion is rarely tabulated in the literature, by this reason we have included two other structural parameters: φ to show the smallest dihedral angle between the Br–Cu–Br planes (90° for tetrahedral and 0° for square-planar geometry) and θ which represents the mean values of the two largest Br–Cu–Br angles. Obviously, the three parameters ΔD, φ and θ carry with them the same information. The results in Table 4 show that the hydrogen-bond effect is controversial. For example, the distortions of $[5\text{-Hamp}]_2[CuBr_4]$ and $[NMe(CH_2CH_2Ph)H_2]_2[CuBr_4]$, both with hydrogen bonds involving the bromine atoms, are the highest observed, but the compounds $[H_2bpipz][CuBr_4]$ and $[H_2bzim][CuBr_4]$ which also possess hydrogen bonds show the smallest distortion. Moreover one of the compounds, $[PMe_4][CuBr_4]$,[29] with no hydrogen bonds has a distortion among the highest found. Accordingly, we may conclude that distortion from T_d geometry is frequently, or at least partly, due to hydrogen-bond interactions, but geometric packing, host-lattice induced distortions, van der Waals contacts and other large electronic effects all play an important role. Hydrogen bonding can act in concert with the other effects or in the opposite direction leading to either an increase or decrease in distortion.[22]

ESR spectroscopy and magnetic susceptibility

The X- and Q-band ESR spectra of a polycrystalline sample of both compounds have been recorded in the range 4.2–300 K. No significant variations were observed over this range of temperature. The signal, $\Delta M_s = \pm 1$, of compound **1** is isotropic with a *g* tensor value of 2.141 [Fig. 5(*a*)]. The signal widths vary in the range 210–225 G, being much narrower than those obtained from $[Hapy]_2[CuBr_4]\cdot H_2O$.[9b] For **2**, axial reversed spectra were obtained at all temperatures, with $g_\perp = 2.045$, $g_\perp = 2.194$, $\langle g \rangle = 2.14$, and a signal width of 242 G at 300 K [Fig. 5(*b*)]. When the temperature was lowered only a narrower signal was recorded. In an attempt to resolve the spectra, Q-band ESR spectroscopy was used. No changes were observed for **2**, but the spectrum of **1** [Fig. 5(*a*)] shows a rhombic-type signal, which remained practically unchanged over the whole range of temperature, with $g_1 = 2.221$, $g_2 = 2.132$ and $g_3 = 2.073$ ($\langle g \rangle = 2.14$). This rhombic signal contrasts with the axial-type Q-band spectra observed for other bromocuprates. In principle, it is due to the high asymmetry in the complex anion, but another origin is also possible. Taking into account the existence of magnetically inequivalent copper(II) ions in **1**, the observed signal could be due to an exchange *g* tensor instead of the molecular tensor. This fact might be also the origin of the reversed axial spectra of **2**.[30] Single-crystal experiments would be necessary to confirm this hypothesis, but unfortunately the size of our crystals is too small for this purpose.

Table 4 Distortion from regular tetrahedral geometry for $[CuBr_4]^{2-}$ complexes

Compound[a]	ΔD (%)[b]	Hydrogen bonds	θ[c]/°	φ[d]/°	Ref.
$[H_2bpipz][CuBr_4]$	7.9	Yes	118.9	80.4	6(*e*)
$[H_2bzim]_2[CuBr_4]$	9.5	Yes	120.8	78.2	6(*f*)
$[NMe_4][CuBr_4]$	13.8	No	125.0	72.7	6(*c*)
$[Cu([17]aneN_5)][CuBr_4]$	15.0	Possible	126.0	71.8	6(*h*)
$[H_3L][CuBr_3][CuBr_4]$	18.5	Yes	128.8	65.5	22
$[H_2en]_2[CuBr_4]$	18.7	Yes	129.6	69.6	6(*b*)
$Cs_2[CuBr_4]$	19.7	No	128.4	71.8	6(*a*)
[Habmp][3-Hamp][$CuBr_4$]	21.0	Yes	131.3	65.5	23(*a*)
$[NPr^i_2H_2][CuBr_4]$	21.2	Yes	135.0	61.2	6(*d*)
$[Hapy]_2[CuBr_4]\cdot H_2O$	22.2	Yes	132.6	63.8	9(*b*)
$[PMe_4]_2[CuBr_4]$	22.9	No	133.2	63.3	29
$[PMe_4]_2[CuBr_4]$[e]	23.0	No	132.6	63.1	29
2	24.1	Yes	132.6	63.9	This work
$[5\text{-Hamp}]_2[CuBr_4]$	27.8	Yes	137.1	56.1	28(*a*)
$[NMe(CH_2CH_2Ph)H_2]_2[CuBr_4]$	34.3	Yes	142.1	51.9	6(*e*)

[a] bpipz = *N*-Benzylpiperazine, bzim = benzimidazole, [17]aneN$_5$ = 1,4,7,11,14-pentaazacycloheptadecane, L = 6-amino-5-(2-carboxyphenylazo)-1,3-dimethyluracil, en = ethane-1,2-diamine, abmp = 2-amino-5-bromo-3-methylpyridine, 3-amp = 2-amino-3-methylpyridine, apy = 4-aminopyridine, 5-amp = 2-amino-5-methylpyridine. [b] Calculated according to ΔD (%) = $1/n\ \Sigma_j|\Sigma_i(\delta_i - \delta_{j1})|/|(\delta_{j1} - \delta_{j2})| \times 100$ where δ_i is the experimental dihedral angle and δ_{j1} and δ_{j2} are the theoretical dihedral angles for T_d and D_{4h} symmetry respectively. [c] Average value of the *trans* L–Cu–L angles (L = Br or N). [d] Dihedral angle between L–Cu–L planes (L = Br or N) (ideal tetrahedron: 90°). [e] The compound contains two crystallographically independent anions.

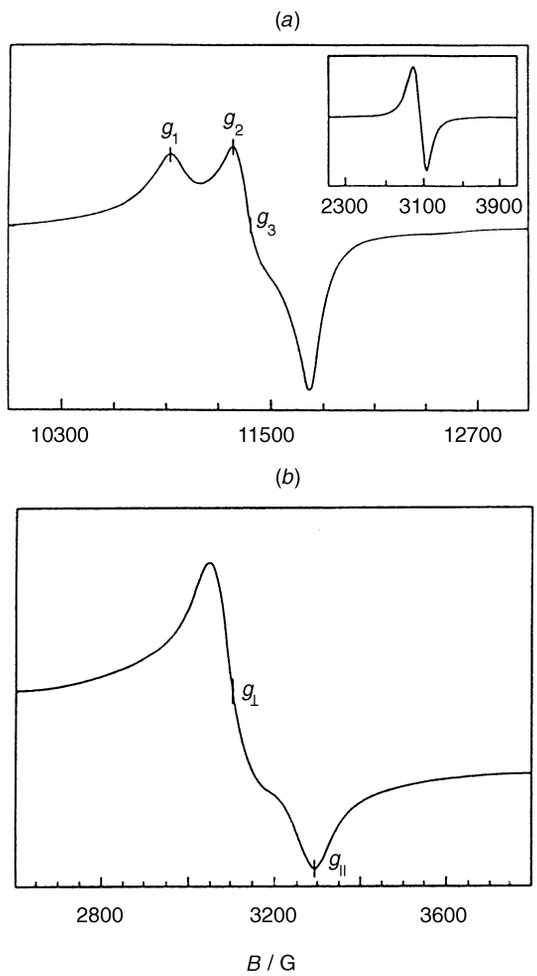

Fig. 5 Q-Band ESR spectra at 100 K for compounds **1** (*a*) and **2** (*b*). Inset: X-band ESR spectrum of **1**

The magnetic susceptibility data for the complexes have been measured over the temperature range 4.2–300 K. The experimental data, plotted as the thermal variation of the reciprocal susceptibility and the $\chi_m T$ product, are shown in Fig. 6. For both compounds the susceptibility follows a Curie–Weiss law at >50 K, with $C = 0.43$ cm^3 K mol^{-1} and $\theta = -2.3$ K for **1** and

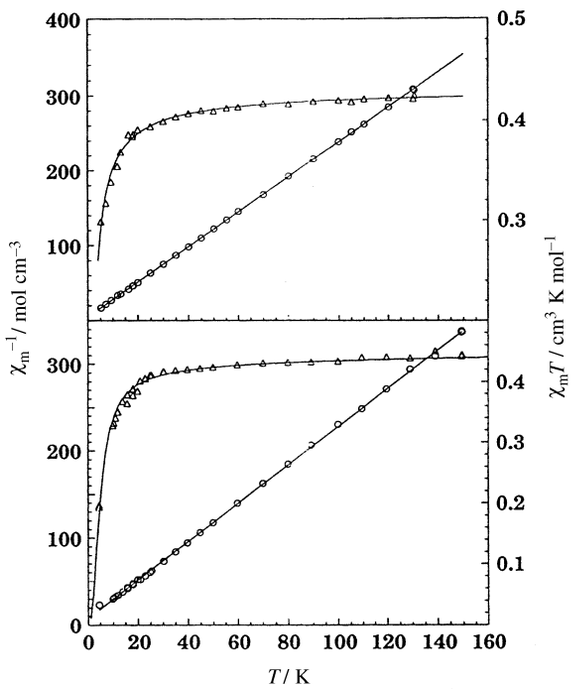

Fig. 6 Thermal variation of the reciprocal magnetic susceptibility and χT for $[C_5H_7N_2][CuBr_3(C_5H_5BrN_2)]$ **1** (top) and $[C_5H_7N_2]_2[CuBr_4]$ **2** (bottom)

$C = 0.46$ cm^3 K mol^{-1} and $\theta = -4.8$ K for **2**. The overall appearance of the $\chi_m T$ *versus* T curves is indicative of weak antiferromagnetic interactions between the copper(II) centres [$\mu_{eff} = 1.84\ \mu_B$ at room temperature (r.t.) and $1.44\ \mu_B$ at 4.2 K for **1** and $\mu_{eff} = 1.88\ \mu_B$ at r.t. and $1.24\ \mu_B$ at 4.2 K for **2**].

Taking into account the structural characteristics of the compounds, the magnetic interaction can only be propagated *via* the hydrogen-bond system. The data were analysed using the Heisenberg model with exchange interaction between pairs of copper(II) ions with spins S_i and S_j, equation (1). We

$$H = \sum_{i>j} -2J_{ij}S_iS_j \qquad (1)$$

assumed interactions between nearest-neighbour copper ions on a chain (*i.e.*, $J_{ij} = J$ for $j = i \pm 1$ and $J_{ij} = 0$ otherwise).

In order to evaluate the magnitude of the exchange coupling constant we used the polynomial expression developed by Hall[31] to describe the results graphically presented by Bonner and Fisher[32] for a uniformly spaced chain of spins $S = \frac{1}{2}$ [equation (2)], where $x = |J|/kT$, N and k are the Avogadro and

$$\chi = \frac{Ng^2\beta^2}{kT}\left(\frac{A + Bx + Cx^2}{1 + Dx + Ex^2 + Fx^3}\right) \qquad (2)$$

Boltzmann constants, β is the Bohr magneton, $A = 0.250$, $B = 0.150$, $C = 0.3009$, $D = 1.9862$, $E = 0.6885$ and $F = 6.0626$.

The solid lines in Fig. 6 are the best least-squares fit of equation (2) to the experimental data with the magnetic parameters $J = -1.20$ cm^{-1} ($J/k = -1.7$ K) and $g = 2.14$ for complex **1** and $J = -2.43$ cm^{-1} ($J/k = -3.5$ K) and $g = 2.16$ for **2**. The agreement factor, defined as $S = [\Phi/(n - K)]^{\frac{1}{2}}$, where n is the number of data points, K the number of parameters, and $\Phi = \Sigma[\chi_m T_{obs} - \chi_m T_{calc}]^2$ is the sum of the squares of the residuals, is equal to 4×10^{-3} for **1** and 3×10^{-4} for **2**. The resulting exchange coupling constants show that the magnetic interactions are slightly stronger in **2** than those in **1**. In **2** adjacent anions are joined through two bridging cations, giving rise to one-dimensional chain of copper(II) ions. In **1** the magnetic interactions are similar to those in **2**, but the coupling pathway presumably involves a longer hydrogen-bond system, which holds adjacent anions together in the one-dimensional zigzag $[C_5H_7N_2]^+$–$[CuBr_3(C_5H_5BrN_2)]^-$ chains. It is possible that there is a small contribution to the magnetic-coupling from the π interaction between the aromatic rings.

The calculated g and J values are in good agreement with those deduced from the ESR spectra and Curie–Weiss fit, respectively. At high temperatures ($|J|/kT \ll 1$) equation (2) becomes a Curie–Weiss law with $\theta = 1.38\ J/k$, and from the observed θ values (−2.3 and −4.8 K) exchange parameters $J/k = -1.67$ and −3.49 K are expected, practically the calculated ones. Therefore, as expected, the one-dimensional Heisenberg model gives a good representation of the magnetic behaviour of these compounds.

Thermal behaviour

The thermal behaviour of both compounds has been deduced from their TG/DTA and DSC curves in both synthetic air and dinitrogen atmospheres (SUP 57207). An outstanding feature in the thermal degradation of **1** is a small endothermic peak that can be seen in the temperature range 85–100 °C (minimum at 95 °C), which has been assigned to a phase transition, TG analysis showing no weight change at this point. The total heat of the transformation, $\Delta H = 3$ kJ mol^{-1}, is in good agreement with those previously found for other crystalline phase transitions.[33] It was not possible to analyse structurally this phase transition since the compound rapidly melted at 125 °C (ΔH for fusion 21 kJ mol^{-1}). No structural phase transitions were observed in the thermal evolution of compound **2** which is stable up to 145 °C at which temperature it melts with a ΔH of 21 kJ mol^{-1}. The phase transition in **1** and the melting processes for both compounds do not show a significant dependence on the nature of the environmental gas, but the decomposition pathways of the liquid and the final residues are affected by the surrounding atmosphere. In air the compounds decompose endothermically with oxidation of the organic units to give copper(II) bromide followed by a strong exothermic loss of bromine to give copper(II) oxide as the final product at >610 °C. No other peak belonging to Cu or another copper oxide was found in the X-ray powder diffractogram of the final stable residue. In nitrogen, all degradation processes are endothermic and lead, without intermediate stable species, to powdered metallic copper as final product at >700 °C. No peaks corresponding to $CuBr_2$ or CuBr could be identified. These results suggest that organic cation pyrolysis under an inert atmosphere can result, direct or indirectly, in reduction of Cu^{II} to Cu^0. Some authors have suggested that the thermal degradation of organoammonium halogenometalate complexes in inert atmospheres is an excellent method of obtaining powdered metal of high reactivity.[34]

Acknowledgements

We thank the Universidad del País Vasco/Euskal Herriko Unibertsitatea (UPV/EHU) (Grant No. UPV 169.310-EA059/96) for financial support. J. S. thanks the Ministerio de Educación y Ciencia of the Spanish Government for a doctoral fellowship (Grant. No. AP94.42172547).

References

1 R. D. Willett, *Coord. Chem. Rev.*, 1991, **109**, 181; L. Subramanian and R. Hoffmann, *Inorg. Chem.*, 1992, **31**, 1021.
2 (*a*) R. D. Willett, H. Place and M. Middleton, *J. Am. Chem. Soc.*, 1988, **11**, 8639; (*b*) B. J. Hathaway, *Structure Bonding* (*Berlin*), 1984, **57**, 55; (*c*) M. A. Romero, J. M. Salas, M. Quirós, M. P. Sánchez, J. Romero and D. Martín, *Inorg. Chem.*, 1994, **33**, 5477.
3 J. Blanchette and R. D. Willett, *Inorg. Chem.*, 1988, **27**, 843; *Magneto-Structural Correlations in Exchange Coupled Systems*, eds. R. D. Willett, D. Gatteschi and O. Kahn, Nato ASI Series, D. Reidel, Dordrecht, 1985, vol. 140.
4 D. Frechilla, B. Lasheras, M. Ucelay, E. Parrondo, G. Craciunescu and E. Cenarruzabeitia, *Arzneim. Forsch. Drug. Res.*, 1991, **41**, 247.
5 D. G. Craciunescu, M. T. Gutiérrez-Ríos, E. Parrondo-Iglesias, C. Molina, A. Doadrio-López, E. Gastón de Iriarte and C. Guirvu, *An. R. Acad. Farm.*, 1989, **55**, 329.
6 (*a*) B. Morosin and E. C. Lingafelter, *Acta Crystallogr.*, 1960, **13**, 807; (*b*) D. N. Anderson and R. D. Willett, *Inorg. Chim. Acta*, 1971, **5**, 41; (*c*) P. Trouelan, J. Lefebvre and P. Derollez, *Acta Crystallogr., Sect. C*, 1984, **40**, 386; (*d*) V. Fernández, M. Morán, M. T. Gutiérrez-Ríos, C. Foces-Foces and F. H. Cano, *Inorg. Chim. Acta*, 1987, **128**, 239; (*e*) H. Place and R. D. Willett, *Acta Crystallogr., Sect. C*, 1988, **44**, 34; (*f*) A. Tosik and M. Bukawska-Strzyzewska, *J. Crystallogr. Spectrosc. Res.*, 1989, **19**, 707; (*g*) T. Manfredini, G. C. Pellacani, A. Bonamartini-Corradi, L. P. Battaglia, G. G. T. Guarini, J. G. Giusti, G. Pon, R. D. Willett and D. X. West, *Inorg. Chem.*, 1990, **29**, 2221; (*h*) J. C. Boeyens, S. M. Dobson and E. L. Oosthuizen, *J. Crystallogr. Spectrosc. Res.*, 1990, **20**, 407.
7 P. C. Healy, C. Pakawatchai and A. H. White, *Aust. J. Chem.*, 1985, **38**, 669; J. M. Savariault, J. Galy, J. M. Gutiérrez-Zorrilla and P. Román, *J. Mol. Struct.*, 1988, 313.
8 M. M. Thackeray and L. R. Nassimbeni, *Acta Crystallogr., Sect. B*, 1974, **30**, 2469.
9 (*a*) P. Román, L. Luque and J. A. Pozo, *Mater. Res. Bull.*, 1992, **27**, 989; (*b*) P. Román, J. Sertucha, A. Luque, L. Lezama and T. Rojo, *Polyhedron*, 1996, **15**, 1253.
10 P. Román and J. M. Gutiérrez-Zorrilla, *J. Chem. Educ.*, 1985, **62**, 167.
11 *Powder Diffraction File of the Joint Committee on Powder Diffraction Standards*, International Center of Diffraction Data, Swarthmore, PA, 1982, Sets 1–32.
12 A. Earnshaw, *Introduction to Magnetochemistry*, Academic Press, London, New York, 1968.
13 K. Iron, W. Jeitschko and E. Parthe, LAZY PULVERIX, Laboratoire de Crystallographie aux rayons-X, Universite of Geneve, Geneve, 1977.
14 N. Walker and D. Stuart, *Acta Crystallogr., Sect. A*, 1983, **39**, 158.
15 *International Tables for X-Ray Crystallography*, Kynoch Press, Birmingham, 1974, vol. 4, pp. 71–79, 149.
16 P. T. Beurskens, G. Admiraal, G. Beurskens, W. P. Bosman, S. García-Granda, R. O. Gould, J. M. M. Smith and C. Smykalla, The DIRDIF program system, Technical Report of the Crystallography Laboratory, University of Nijmegen, 1992.
17 J. M. Stewart, P. A. Machin, C. W. Dickinson, H. L. Ammon, H. Heck and H. Flack, The X-RAY 76 System, Technical report TR-446, Computer Science Center, University of Maryland, College Park, Maryland, 1976.
18 M. Martínez-Ripoll and F. H. Cano, PESOS, Instituto Rocasolano, CSIC, Madrid, 1975.
19 A. L. Spek, *Acta Crystallogr., Sect. A*, 1990, **46**, C34.

20 *CRC Handbook of Chemistry and Physics*, 59th edn., eds. R. C. Weast and M. J. Astle, CRC Press, Boca Raton, FL, 1978.
21 P. S. Braterman, *Inorg. Chem.*, 1963, **2**, 448; G. Marcotrigiano, L. Menabue and G. C. Pellacani, *Inorg. Chem.*, 1970, **5**, 2333; G. Marcotrigiano, L. Menabue, G. C. Pellacani and M. Saladini, *Inorg. Chim. Acta*, 1979, **34**, 43; P. Stein, P. W. Jensen and T. G. Spiro, *Chem. Phys. Lett.*, 1981, **80**, 451.
22 M. R. Sunberg, R. Kivekäs, J. Ruiz, J. M. Moreno and E. Colacio, *Inorg. Chem.*, 1992, **31**, 1062.
23 (*a*) H. Place and R. D. Willett, *Acta Crystallogr., Sect. C*, 1987, **43**, 1497; (*b*) T. E. Grigereit, B. L. Ramakrishna, H. Place, R. D. Willett, G. C. Pellacani, T. Manfredini, L. Menabue, A. Bonamartini and L. Battaglia, *Inorg. Chem.*, 1987, **26**, 2235.
24 R. D. Willett and K. Halvorson, *Acta Crystallogr., Sect. C*, 1988, **44**, 2068.
25 E. L. Muetterties and L. J. Guggenberg, *J. Am. Chem. Soc.*, 1974, **96**, 1749.
26 F. H. Allen, O. Kennard, D. G. Watson, L. Brammer, A. G. Orpen and R. Taylor, *J. Chem. Soc., Perkin Trans.* 2, 1987, S1.
27 P. Pelikán and M. Liska, *Collect. Czech. Chem. Commun.*, 1984, **49**, 2837.
28 (*a*) H. Place and R. D. Willett, *Acta Crysallogr., Sect. C*, 1987, **43**, 1050; (*b*) D. Reinen, M. Atanasov, G. S. Nicolov and F. Steffens, *Inorg. Chem.*, 1988, **27**, 1678.
29 G. Madariaga, M. M. Alberdi and F. J. Zuñiga, *Acta Crystallogr., Sect. C*, 1990, **46**, 2363.
30 B. J. Hathaway and D. E. Billing, *Coord. Chem. Rev.*, 1970, **5**, 143; W. E. Estes, D. P. Gavel, W. E. Hatfield and D. J. Hodgson, *Inorg. Chem.*, 1978, **17**, 1415.
31 J. W. Hall, Ph.D. Thesis, University of North Carolina, 1977.
32 J. C. Bonner and M. E. Fisher, *Phys. Rev., A*, 1964, **135**, 640.
33 W. W. Wendlant, *Thermal Analysis*, 3rd edn., Wiley, New York, 1986.
34 J. R. Allan, *Thermochim. Acta*, 1992, **200**, 355 and refs. therein.

Received 17*th September* 1996; *Paper* 6/06429I